J. Mol. Biol. (1972) **71**, 363–381

The Topography of Lambda DNA: Isolation of Ordered Fragments and the Physical Mapping of Point Mutations

J. Barry Egan† and David S. Hogness

Department of Biochemistry
Stanford University School of Medicine
Stanford, Calif. 94305, U.S.A.

(*Received 16 March 1972*)

The members of a set of overlapping fragments of λ DNA have been isolated. The set is divided into two groups, the right and left families. All members of the right family contain the cohesive site at the right end of λ DNA; members of the left family contain the cohesive site at the left end. The members of each family differ in molecular length and this characteristic was used to order and to isolate the fragments. Each family is comparable to an ordered set of overlapping deletions and the principles of deletion mapping can therefore be applied to both chemically and genetically defined characteristics of λ DNA.

Mapping of mutant loci is possible because (1) all fragments in a family are active in the Kaiser–Hogness helper phage assay for genetic activity, and (2) the distance between a given locus and that end of λ DNA defining the family is equal to the length of the shortest fragment which contains the locus. The lengths of such fragments were determined from their sedimentation coefficients to yield the following positions for six amber mutations, expressed as f_R, the fraction of the length of whole λ DNA measured from the right end: *N*7, 0·268; *O*29, 0·214; *P*80, 0·186; *Q*21, 0·090; *R*54, 0·55; *R*221, 0·052. The left boundary of the imm^{λ}/imm^{434} non-homology region was mapped at $f_R = 0{\cdot}252$.

The advantage of the mapping methods described here is that they are applicable to point mutations and to characteristics which can be defined by direct chemical analysis of the DNA. In the following paper (Champoux & Hogness, 1972), the position and orientation of the ten specific sequences which generate poly(rG) binding sites and the topography of base composition in λ DNA were determined.

1. Introduction

The problem that we pose here is the isolation of the members of an ordered set of fragments of λ DNA which allow both chemical and genetic mapping of the genome in physical units. The set we have chosen consists of two families of fragments, the right and left families. A necessary and sufficient condition for a fragment to be a member of a given family is that it contain the corresponding cohesive site (Hershey, Burgi & Ingraham, 1963). Figure 1 contains a diagram illustrating this definition.

The members of a given family are comparable to a set of overlapping deletions to which the principles of deletion mapping can be applied. Since the gene contents of all members can be determined by the helper-assay of Kaiser & Hogness (1960), the

† Present address: Department of Biochemistry, University of Adelaide, Adelaide, South Australia 5001, Australia.

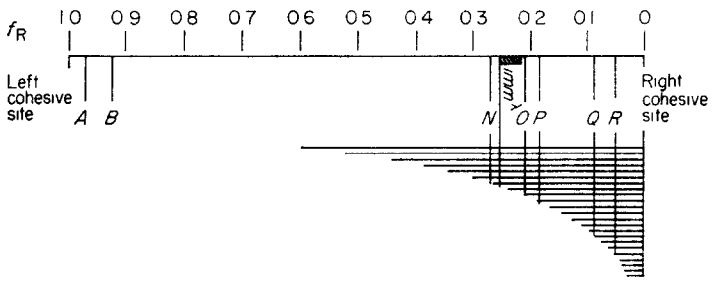

FIG. 1. Schematic defining the fragments of the right family.

The horizontal lines represent the duplex DNA of whole molecules (top line) and fragments in the right family; the lengths are given as the fraction of whole λ DNA measured from the right end (f_R). The fragments have been drawn so that the ratio of lengths between adjacent members is kept constant, a characteristic of the fractionation procedure. A cohesive site is a single-strand extension of 12 bases, the strand and sequence of the left site being complementary to that in the right site (Wu & Taylor, 1971). The amber mutations used in this paper are located in the genes indicated by the capital letters, the positions being taken from our data (except for *A* and *B*, which derive from Davidson & Szybalski, 1971); *imm*$^\lambda$ is the immunity region of λ and our determination of its left boundary is indicated.

position of a given gene can be determined from the genetic differences between adjacent members and their molecular lengths. Chemical mapping of the genome can be accomplished by a similar analysis of differences for any characteristic which can be analyzed. The entire λ DNA molecule can be mapped if the largest fragment in each family is at least one-half the molecular length of the whole λ DNA molecule. In practice the largest member of a family is the largest fragment in the population of corresponding "halves" (Hogness & Simmons, 1964), which has been shown to be greater than one-half the length of whole λ DNA (Hogness, 1966).

In this paper, we describe the method for isolating the members of the right family, and order these fragments with respect to size and gene content, thereby determining the physical location of several point mutations in the right half of λ DNA. In the succeeding paper (Champoux & Hogness, 1972), these fragments are used to map both the base composition and the poly(rG) binding sites on both strands of λ DNA.

2. Experimental Procedure

(a) *Materials*

(i) *Media*

The TB, TB soft agar and TB plate agar have been described by Kaiser & Hogness (1960), and TCM by Kaiser & Inman (1965). The E34 medium consists of 56 mM-Na_2HPO_4, 22 mM-KH_2PO_4, 19 mM-NH_4Cl, 8·6 mM-NaCl, 0·04 mM-$FeSO_4$, 10 mM-$MgSO_4$ to which glucose (0·5 mg/ml.), vitamin B_1 (10 μg/ml.), Difco Casamino acids (0·5 mg/ml.) and thymidine (2 μg/ml.) were added. E34a medium is E34 without thymidine to which xanthine (25 μg/ml.) and uridine (20 μg/ml.) were added, and the Casamino acids content raised to 6 mg/ml. All organic components were sterilized by filtration (Millipore) of concentrated stock solutions, the Casamino acids being treated with an equal weight of Norit A for 24 hr at 0 to 4°C before sterilization.

(ii) *Phage and bacteria*

The source of all DNA preparation was *λind⁻cI857* (Sussman & Jacob, 1962). The helper phage used in the genetic assays are given in Table 1.

The following characteristics of the *Escherichia coli* K12 strains are relevant to their use here: C600 (Appleyard, 1954) and R⁻A9605 *sup*⁺3 (Yanofsky & Ito, 1966) contain the amber suppressors *sup*⁺2 and *sup*⁺3, respectively; W3350 (Campbell, 1961) is *sup*⁻; and CR34 (*λind*⁻*cI*857)/λ is a thymine-requiring lysogen (Baldwin, Barrand, Fritsch, Goldthwait & Jacob, 1966) resistant to λ infection. Lysogenic derivatives of C600 and W3350 were isolated from survivors of phage infection.

(iii) *Special reagents*

CsCl (Harshaw Chemical Co.) was selected for low levels of contamination by heavy-metal cations as described by Doerfler & Hogness (1968). Cs_2SO_4 (S. Cohen Associates) was selected because it contained the least amount of Hg(II) complexants among commercial sources tested. Solutions of sucrose (Mann, enzyme grade) were treated with Norit A before use in zone sedimentations.

(b) *Methods*

(i) *Assays*

Infective phage were assayed as plaque-forming units on C600 bacteria (Hogness & Simmons, 1964).

Genetic activities of DNA were assayed according to Kaiser & Inman (1965) with the following modifications: (1) adsorption of the helper phage occurred during 15 min at 0°C; (2) the complexes were incubated for 10 min at 37°C; (3) the helper-infected bacteria were stored over liquid nitrogen and thawed as described by Hogness & Simmons (1964); (4) in the assay, 0·1 ml. of helper-infected bacteria in TCM (2×10^9/ml.) were mixed with 0·1 ml. of DNA in TCM and pancreatic DNase in TCM was added (final concentration of 10 μg/ml.) after 25 min of incubation at 37°C, and incubation continued for a further 5 min. The helper phage, recipient bacteria, and indicator bacteria used in each assay are given in Table 1. The specific activity for any gene combination is the number of plaques obtained in the assay, divided by the μg of DNA required to obtain them, expressed as plaque-forming units/μg.

(ii) *Isolation of phage and DNA*

The helper phage (Table 1) were obtained either from plate stocks grown on C600 or from lysates of C600 lysogens induced by ultraviolet light, and were purified by sedimentation in CsCl gradients (Doerfler & Hogness, 1968).

Phage used as the source of λ DNA were prepared by heat induction of 100-l. batches of W3350 (*λind*⁻*cI*857) at a concentration of 7×10^8 bacteria/ml. of Difco Penassay broth, induction being effected by raising the temperature from 34 to 45°C (5 min to achieve this increase, 4 min at 45°C) and then lowering it to 37°C where it was maintained until lysis was complete. The phage were purified as described by Doerfler & Hogness (1968), except that they were concentrated from the lysate by polyethylene glycol/sodium dextran sulfate phase separation as described by Casjens, Hohn & Kaiser (1970), and then banded twice in CsCl before dialysis against 0·01 M-$MgCl_2$, 0·05 M-Tris·HCl buffer (pH 7·2).

Phage containing DNA labeled with 5-bromouracil were prepared by heat induction of CR34 (*λind*⁻*cI*857) as described above with the following variations: 5×10^{13} bacteria, grown at 34°C in 100 l. of E34 medium supplemented with 2·0 g of uridine and 2·5 g of xanthine, were harvested by centrifugation, resuspended at 0°C in 2 l. of E34a medium containing 1·0 g of 5-bromouracil, and then added to 48 l. of E34a medium at 47°C; after 5 min at the resulting temperature of 45°C, the culture was cooled to 40°C, allowed to lyse, and the phage purified as above except that the density of the CsCl solution was raised to 1·55 g/ml.

DNA was prepared from both types of phage according to the method of Kaiser & Hogness (1960) except that: (1) the phenol was saturated with 0·01 M-EDTA, 1·0 M-Tris·HCl buffer (pH 8·0), (2) the phenolic phase residues were extracted with 0·001 M-EDTA, 0·01 M-Tris·HCl buffer (pH 7·5) and (3) the combined aqueous phases containing the DNA were dialyzed against 0·01 M-Na_2SO_4, 0·005 M-$Na_2B_4O_7$ (pH 9·0). All DNA preparations had 80 to 100% of the strands intact (Doerfler & Hogness, 1968).

TABLE 1

Components for genetic assays of DNA

Components of the assay	Combinations of λ genes assayed								
	A,B	imm^{λ}	*A,B,*imm^{λ}	*N,R*	imm^{λ}*,R*	*O,R*	*P,R*	*Q,R*	*R*
Amber mutations in the λimm^{434} helper phage†	*A32B1*	*A32B1*	*A32B1*	*N7R60*	*R54,60*	*O29R60*	*P80R60*	*Q21R60*	*R54,60*
Recipient bacteria	R⁻A9605 *sup*⁺3	R⁻A9605 *sup*⁺3	R⁻A9605 *sup*⁺3	C600 *sup*⁺2	W3350	W3350	W3350	W3350	W3350
Indicator bacteria‡	W3350	C600 (λimm^{434})	W3350 (λimm^{434}*A32B1*)	W3350	C600 (λimm^{434})	W3350	W3350	W3350	W3350

† The numbers represent the *sus* mutation numbers assigned by Campbell (1961). The phage containing *A32B1* has been described by Kaiser & Inman (1965) and contains a *cI*-type mutation, *c*, in the imm^{434} region; those containing *N7R60*, *O29R60*, or *P80R60* are recombinants from λ *R60* crossed to imm^{434} (the 434hy of Kaiser & Jacob, 1957) carrying the appropriate *N*, *O* or *P* mutations; that containing *R54,60* was derived from recombination between λimm^{434} and $\lambda imm^{434}cR54,60$ (isolated by Kaiser) to replace $imm^{434}c$ with imm^{434}; and that containing *Q21R60* was obtained from Kaiser directly.

‡ Either the entire assay mixture (0·3 ml.; see text) or one-tenth of it (0·3 ml. of a 10-fold dilution of the reaction mixture in TCM) was mixed with 0·2 ml. of indicator bacteria in TB at a density of 1×10^9/ml. and 2 ml. of TB soft agar, and poured on TB plates.

(iii) *Shearing of λ DNA*

DNA was sheared according to the method of Hogness & Simmons (1964) with the following variations. At the high concentrations of 50, 200, and 275 μg whole λ DNA/ml. in the above borate buffer, the stirring speed required to break ≥ 98% of the molecules to halves in 120 min is 1700, 2750, and 2950 rev./min, respectively, breakage being followed both by the decrease in reduced viscosity and by loss of the *A,B-imm*$^{\lambda}$-linked activity (Hogness & Simmons, 1964). Shearing of isolated right halves to smaller fragments by stirring at higher speeds was performed similarly except that the DNA concentration was always 50 μg/ml., the solvent, 0·001 M-EDTA, 0·01 M-Tris·HCl (pH 7·1), and the time of stirring generally shorter (see legend, Table 2).

(iv) *Isolation of halves*

Right and left halves of λ DNA were isolated by sedimentation in Hg(II)–Cs_2SO_4 solutions (Wang, Nandi, Hogness & Davidson, 1965), using a molar ratio of Hg(II) to DNA phosphorus of 0·28, and a solution density of 1·61 g/ml. for initial DNA concentrations ≥ 20 μg/ml.; for lower DNA concentrations (0·8 to 20 μg/ml.), the solution density was varied between 1·51 and 1·61 g/ml. to ensure that the bands of halves occupied the center of the tube. Centrifugation conditions: 40 hr at 45,000 rev./min and 4°C in the Spinco model 50 rotor. The halves of bromouracil-labeled λ DNA were isolated by the same method except that the solution density was increased by 0·04 g/ml. A fractionation pattern for labeled halves is given in Figure 2, along with genetic data indicating that cross contamination of the halves can be kept well below the 2% level maintained as the upper limit for all preparations. After isolation, all preparations were dialyzed against 0·001 M-EDTA, 0·01 M-Tris·HCl (pH 7·1) at 0 to 4°C.

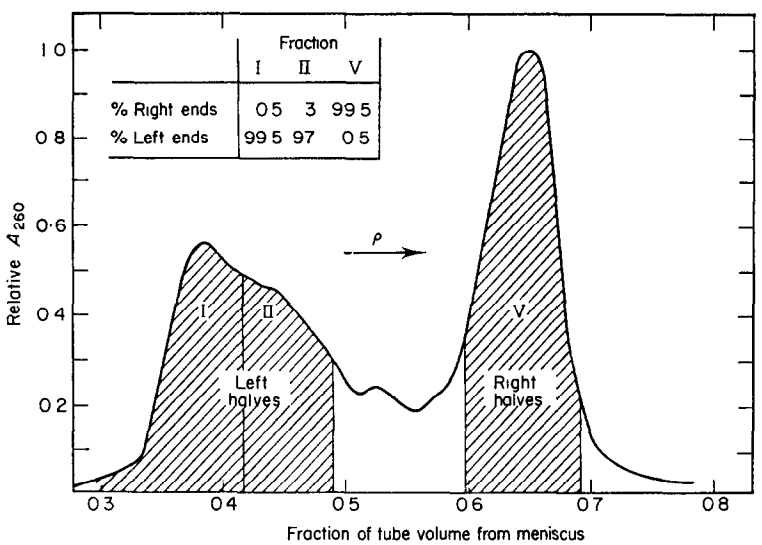

FIG. 2. Hg(II)–Cs_2SO_4 equilibrium centrifugation of 5-bromouracil-labeled halves.

Bromouracil-labeled λ DNA was stirred and then centrifuged to equilibrium in Hg(II)–Cs_2SO_4 as described in Experimental Procedure. The relative $A_{260\,nm}$ values are taken from a continuous trace recorded during collection and fractionation of the gradient (see section (b), Experimental Procedure). The DNA recovered in fractions I, II and V represents, respectively, 19, 15 and 33% of the total DNA centrifuged. The inset shows the percentage distribution of left and right half-molecules within each of these fractions as determined by gene assay for left (*A,B*) and right (*imm*$^{\lambda}$) markers. The linked *A,B-imm*$^{\lambda}$ activity due to whole molecules was negligible in these fractions. The total activity of *imm*$^{\lambda}$ in fractions I or II, divided by the specific activity of *imm*$^{\lambda}$ in fraction V yields the amount of contaminating DNA in I or II. Similarly the total activity of *A,B* in V divided by the specific activity of *A,B* in I determines the contaminating DNA in V.

(v) *Hybrid formation between 5-bromouracil-labeled left halves and fragments of the right family.*

The above right halves (or populations of smaller fragments derived from them) were concentrated to $A_{260\,nm} = 4{\cdot}5$ by rotary evaporation, 5 M-NaCl added to a final concentration of 0·6 M, and incubated at 50°C for 1 hr to allow any contaminating fragments containing left cohesive sites to cohere to the right cohesive sites. Bromouracil-labeled left halves (1·1 vol., $A_{260\,nm} = 5$) in 0·6 M-NaCl, 0·001 M-EDTA, 0·01 M-Tris·HCl (pH 7·1) at 50°C were added to 1 vol. of the preceding solution, and the incubation at 50°C continued for 5 hr. The purpose of the first 1 hr incubation is to eliminate reaction between contaminating fragments containing left cohesive sites and contaminating bromouracil-labeled right halves. After cooling to 23°C, solid CsCl and 0·001 M-EDTA, 0·01 M-Tris·HCl (pH 7·1), were added to the 2·1 vol. of the DNA solution to obtain 3·3 vol. of a solution that is 58·2% (w/w) in CsCl. The hybrids were then isolated from this solution by centrifugation (see Fig. 4).

(vi) *Sedimentation coefficients*

Sedimentation coefficients of DNA were determined by band centrifugation (Vinograd, Bruner, Kent & Weigle, 1963) in the Spinco model E analytical centrifuge equipped with scanner and multiplex accessories under conditions described by Studier (1965), except that the speed and temperature were 36,000 rev./min and 19 to 21°C, and the solvent was sometimes 0·317 M-CsCl instead of 1·0 M-NaCl. All sedimentation coefficients reported here are $S_{20,w}$ values for NaDNA (see Table 1 of Studier (1965) for correction factors in Na-solvents; in 0·317 M-CsCl, the equivalent correction factor is 1·022 as calculated from $\bar{v}$ (Hearst, 1962), η and ρ (Lyons & Riley, 1954; International Critical Tables, 1926 to 1933)). Values of $S^0_{20,w}$ determined in 0·317 M-CsCl (i.e. for CsDNA) were converted to that for NaDNA by dividing by 1·33, the mean of the ratio of $S^0_{20,w}$ for Cs- and NaDNA. (Observed values for the ratio and for $S^0_{20,w}$ of the NaDNA in four fragment populations were 1·35, 15·6 S; 1·33, 17·2 S; 1·34, 20·6 S; 1·31, 25·1 S. Since Bruner & Vinograd (1965) obtained a ratio of 1·33 for T7 DNA which exhibits an $S^0_{20,w}$ of 32·0 S in the Na-form (Freifelder, 1970), the ratio is not dependent upon molecular length in the region of interest here.)

Values of $S^0_{20,w}$ for the DNA in fractions obtained from zone sedimentation in sucrose gradients were either determined directly by band sedimentation in the analytical centrifuge (after dialysis against 0·001 M-EDTA, 0·01 M-Tris·HCl, pH 7·1) or were calculated from the relation $(S^0_{20,w})_1/(S^0_{20,w})_2 = d_1/d_2$ (Martin & Ames, 1961; Burgi & Hershey, 1963), where the subscripts represent two fractions from the sucrose gradient, d is the distance sedimented by the DNA in such fractions, and the value of $S^0_{20,w}$ for the DNA in one of the two fractions (usually the fraction corresponding to the peak of the distribution) is known from analytical band sedimentation. Tests of the latter method indicate that it is reliable to within the reproducibility of $S^0_{20,w}$ determinations by band sedimentation (1 to 2%); e.g. the $S^0_{20,w}$ of the DNA located at 0·566 in the distribution of R9 DNA (Fig. 6) was found to be 12·5 S when determined directly by band sedimentation, and 12·4 S when determined from the relative distances sedimented by DNA in this fraction and in the peak, $S^0_{20,w}$ for the peak DNA being 14·3 S.

(vii) *Calculation of the molecular lengths of fragments*

The molecular lengths of fragments, f (expressed as the fraction of the length of whole λ DNA), were calculated from their sedimentation coefficients according to the equation:

$$f = (4{\cdot}03 \times 10^{-5})(S^0_{20,w})^{2{\cdot}86}. \qquad (1)$$

Equation (1) is derived from the empirical equation $S^0_{20,w} = KM^a$, or $f = [(S^0_{20,w})/(S^0_{20,w})_{\lambda\,DNA}]^{1/a}$, where M is the molecular weight and K and a are constants. The value of a was taken as 0·35 from data in the literature (0·35, Burgi & Hershey, 1963; 0·346, Studier, 1965; 0·350, Leighton & Rubinstein, 1969) and our best fit to the data given in Fig. 3; and $S^0_{20,w}$ for λ DNA was taken as 34·4 S (Freifelder, 1970), which is not significantly different from the value of 34·5 S found by us. Figure 3 contains a plot of f, computed from equation (1), against the corresponding relative molecular weight determined independently by electron microscopy, autoradiography, or light scattering. The deviation of f from the straight line (range = ± 6%) is no greater than expected from errors in the determination

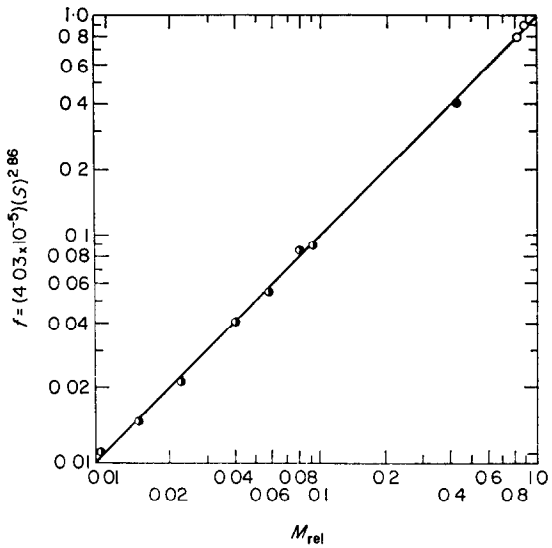

FIG. 3. Correlation between f and relative molecular weights determined independently of $S^0_{20,w}$.

The molecular weights relative to that for λ DNA (M_{rel}) were determined by: (1) relative contour lengths (electron microscopy) of DNA's from λb2 (see Davidson & Szybalski, 1971, for summary) and T7 (data of R. W. Davis & R. W. Hyman, and of D. Lang, cited by Davidson & Szybalski, 1971) (○); (2) autoradiography of T7 halves (Leighton & Rubinstein, 1969) (●); (3) light-scattering (all DNA's listed by Eigner & Doty (1965) in their search of the literature, or determined by them, with molecular weights in the reliable range for light scattering measurements ($<3\times10^6$ daltons) are included) (◑). The molecular weight of λ DNA was taken as $30{\cdot}8\times10^6$ daltons (Davidson & Szybalski, 1971) for the calculation of M_{rel} for classes (2) and (3) above. Values of $S^0_{2,w}$ for the examples in class (3) are given by Eigner & Doty (1965); the value for T7 halves (25·1 s) was calculated from the ratio of its sedimentation coefficient to that for T7 DNA in zone sedimentation (Leighton & Rubinstein, 1969), and the value for T7 DNA (32·0 s; Freifelder, 1970); and the value for λb2 DNA (33·1 s) results from our work.

of $S^0_{20,w}$ (see Discussion for further data confirming equation (1)) nor is a better fit obtained for this range of molecular weights if the more complex relation, $(S^0_{20,w}-b) = KM^a$, is used to calculate f (a, b and K are constants determined empirically by Crothers & Zimm (1965) and by Freifelder (1970)).

(viii) *Absorbance data from preparative centrifugations*

The absorbance at 260 nm ($A_{260\,nm}$) in preparative centrifugations was determined by continuous recording (Gilford model 2000 spectrophotometer) during withdrawal of the solution from the bottom (or top) of the centrifuge tube, accomplished by forcing aqueous solutions of the appropriate density into the top (or bottom) of the tube at a constant rate with a syringe pump (Harvard model 600–900 V).

3. Results

(a) *Formation and isolation of fragments from the right family*

(i) *Experimental plan*

The source of fragments in the right family is the right halves. The term "halves" is a euphemism for a population of fragments created by stirring solutions of whole λ DNA at the minimum speed necessary to break all molecules in a reasonably short time (Hogness & Simmons, 1964). The length distribution of halves has a maximum at

$f = 0{\cdot}5$ (where f is the fraction of the length of whole λ DNA), but is broad because single breaks in wholes occur over the range $f = 0{\cdot}5 \pm 0{\cdot}15$, and is asymmetric because some wholes suffer two breaks (Hogness, 1966). Further breakage of halves to smaller fragments results in length distributions as broad or broader than those for halves (Kaiser & Inman, 1965).

These observations yield three conclusions relevant to the isolation of fragments in the right family; (1) halves are contaminated with internal fragments which lack cohesive sites; (2) controlling the stirring speed allows only a coarse adjustment of molecular length; (3) this adjustment is sufficiently coarse that the complete set of molecular lengths in a family can be generated by application of a small number of different stirring speeds.

After isolation, the right halves are therefore treated in either of two ways. If the desired members of the right family are present in appreciable frequency, these halves are first fractionated to remove internal fragments, and the resulting members of the right family then fractionated according to molecular length by zone sedimentation. If shorter fragments than are provided by halves are desired, the right halves are further fragmented at one of three higher stirring speeds before removal of internal fragments and subsequent fine resolution of molecular length by zone sedimentation.

(ii) *Coarse adjustments of molecular lengths*

Solutions of λ DNA at a concentration of 50 μg/ml. yield halves if stirred at 1700 rev./min (Experimental Procedure, section (b)). Isolated right halves at this same concentration were fragmented further by stirring at 3000, 6000 or 9000 rev./min. Data regarding the size and gene content of these preparations are given in Table 2. The sedimentation coefficients and the molecular lengths derived from these values belong to the fragments appearing at the peak of the sedimentation distribution. Other

TABLE 2

Physical and genetic characteristics of sheared λ DNA

Fragment population†	$S^0_{20,w}$ (s)	f§	Gene content of the population ¶					
			N	*imm*$^{\lambda}$	*O*	*P*	*Q*	*R*
Right halves‡	25·1	0·406	++	++	++	++	++	++
3000	20·9	0·240	+	+	++	++	++	++
6000	17·2	0·127	−	−	−	−	++	++
9000	14·3	0·081	−	−	−	−	+	+

† Right halves were prepared as described in Experimental Procedure, using the highest DNA concentration. The other 3 populations derive from right halves by stirring at the speeds indicated by the number, the time of stirring being 90 min at the highest speed and 30 min at the other two speeds.

‡ The population of right halves characterized here and in Figs 6 and 7 was stirred at a higher speed and DNA concentration than was the case for the population shown in Fig. 4(a), which like that reported by Hogness (1966) exhibits $f = 0{\cdot}50$.

§ f is the fraction of the length of whole λ DNA. It represents molecules in the peak of the sedimentation distribution as it is computed from the $S^0_{20,w}$ value with the aid of equation (1).

¶ Gene activities were assayed as described in Experimental Methods, the designated gene always assayed in combination with *R* (see Table 1). ++ indicates a specific activity ≥30% the value for right halves; + indicates a value 1 to 30% that of right halves; − indicates a value <1% that of right halves.

parameters of these length distributions can be obtained from the data given in the section on fine adjustment of molecular length. The loss of gene activity with decreasing length results from the fact that only fragments with cohesive sites are active in the assay (Kaiser & Inman, 1965). The order in which the genes are lost is that predicted from the genetic linkage map (Campbell, 1971). This correlation represents a rapid method for determining the gene order that has been emphasized previously with regard to the genes of the galactose operon in the left half of λ dg (Hogness, 1966).

(iii) *Removal of contaminating internal fragments*

Each population of fragments given in Table 2 can be divided into two classes: internal fragments and the external fragments containing the right cohesive site. These two classes were fractionated by causing the right cohesive sites of the external fragments to cohere to the left cohesive sites of bromouracil-labeled left halves (see Experimental Procedure section (b)), thereby creating a hybrid molecule with a buoyant density intermediate between the unlabeled and bromouracil-labeled DNA. Separation of these components was accomplished by sedimentation to equilibrium in CsCl gradients as is shown in Figure 4.

Figure 4(a) represents the results from a pilot experiment in which right halves ($f = 0{\cdot}50$) were labeled with tritium so that their distribution throughout the gradient could be determined. The hybrid molecules will vary in density depending upon the relative lengths of the heavy and light fragments; hence a broad density distribution for hybrids is expected from the broad length distribution of halves. The heterogeneity in the hybrid population is indicated by the decrease in the ratio of tritium-labeled DNA to total DNA with increasing density across the hybrid peak. This ratio, normalized to 1·00 for the internal fragments, is 0·52 at the hybrid peak, and 0·62 and 0·38 where the A_{260} is one-half the peak value, to the left and right, respectively. These values indicate that the left and right halves used here have approximately equal length distributions. This equivalence is also indicated by the fact that the ratio of the radial distance between the peaks of bromouracil-labeled DNA and of hybrids ($r_{\mathrm{BrUra}} - r_{\mathrm{hy}}$) to that between the hybrid and internal fragments ($r_{\mathrm{hy}} - r_{\mathrm{i}}$) is 1·02 (Baldwin, 1971).

As the mean length of the fragments in the populations derived from the right halves decreases, the peak of the hybrids must move closer to that for the bromouracil-labeled DNA. This can be observed in Figure 4(b) where the 3000 population of fragments (Table 2) was hybridized. The ratio $(r_{\mathrm{BrUra}} - r_{\mathrm{hy}})/(r_{\mathrm{hy}} - r_{\mathrm{i}})$ in this case is 0·46. The molecular length of the right fragments in the hybrid peak is therefore about one-half that for the bromouracil-labeled left halves (Baldwin, 1971) and is consistent with the assignment of $f = 0{\cdot}24$ for the peak of the 3000 population (Table 2).

The fragments formed by stirring at 6000 and 9000 rev./min form hybrids with densities even closer to that of the bromouracil-labeled DNA so that fractionation of the hybrids from the bromouracil-labeled DNA in the gradient is not useful. However, as the bromouracil-labeled DNA is cleanly separated from the lighter external fragments in the next step (Fig. 5), this prior fractionation is not critical.

The isolation of the right fragments in the hybrids is accomplished by heating to break the 12 base pairs formed by the cohered ends (Wu & Taylor, 1971), followed by centrifugation in a Hg(II)–Cs_2SO_4 gradient to separate the light fragments from the bromouracil-labeled left halves. The result is shown in Figure 5(a). Centrifugation of the Hg(II)–DNA complexes in Cs_2SO_4 is used rather than centrifugation in CsCl,

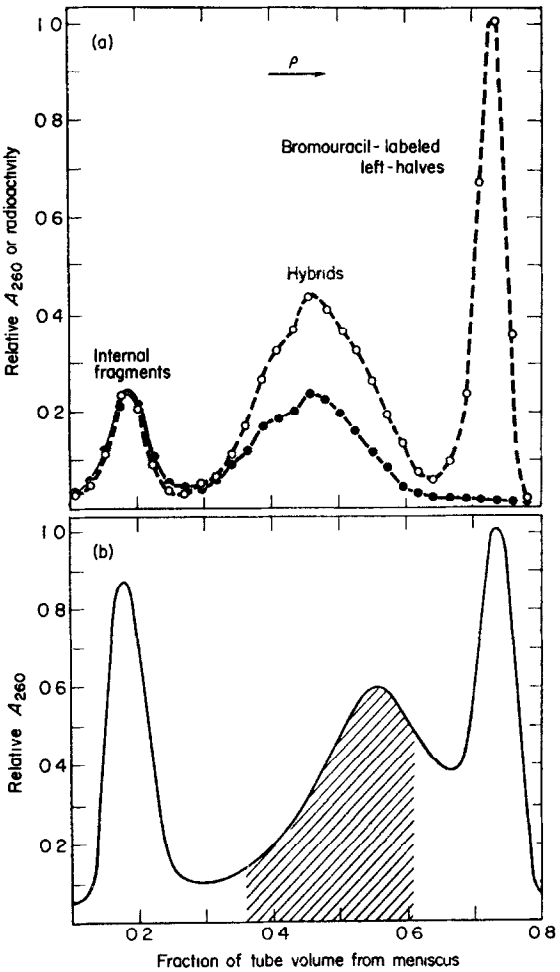

FIG. 4. Equilibrium centrifugation after hybridization of fragments and 5-bromouracil-labeled left halves.

Bromouracil-labeled left halves were mixed with (a) tritium-labeled right halves, or (b) the 3000 fragments (Table 2), incubated to form hybrids, cooled and CsCl added as described in Experimental Procedure. The mixture was then centrifuged at 45,000 rev./min for 60 hr at 23°C in a Spinco model 50 rotor. The peak of internal fragments exhibited insignificant genetic activity, indicating that hybridization was complete (>98%) and that internal fragments are inactive in the helper-phage assay.

(a) Each fraction was assayed for radioactivity (cts/min/ml., —●—●—) and A_{260nm} (--○--○--). The A_{260nm} curve was normalized to 1·0 at the peak of bromouracil-labeled left halves and the curve of radioactivity then normalized so that both curves have the same value for the peak of internal fragments.

(b) The A_{260nm} trace was obtained as in Fig. 2, the shaded area representing the fractions treated to yield the curve given in Fig. 5(a).

because the preferential binding of Hg(II) to single strands (Nandi, Wang & Davidson, 1965), tends to prevent reassociation of the cohesive sites.

As the right fragments have a higher frequency of A·T base pairs than the left halves (for a map of base composition, see Champoux & Hogness, 1972), they take up more Hg(II) than the bromouracil-labeled left halves, and the separation of the two

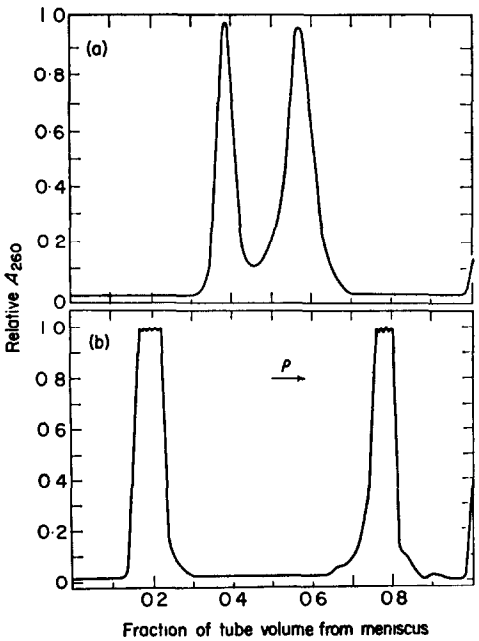

FIG. 5. Separation of the components in the density hybrids by Hg(II)–Cs_2SO_4 equilibrium centrifugation.

(a) The density hybrids from the shaded area in Fig. 4(b) were dialyzed extensively against 0·01 M-Na_2SO_4, 0·005 M-$Na_2B_4O_7$ buffer (pH 9·0), at 0 to 4°C, and heated for 10 min at 64°C to dissociate the cohered components of the hybrid. After cooling rapidly to 0°C, $HgCl_2$ and Cs_2SO_4 were added and the solution centrifuged as described for the fractionation of halves (see Experimental Procedure, section (b)).

(b) A hybrid between unlabeled left halves and bromouracil-labeled right halves was treated as in (a).

components in Figure 5(a) is not as great as it would be if they both had the same base composition. This effect can be seen in Figure 5(b) where the separation of light *left* halves and bromouracil-labeled *right* halves is shown; here the difference in base composition acts in concert with the bromouracil-label to increase the difference in buoyant density of the two species.

(iv) *Fine adjustment of molecular length*

The purified fragments of the right family exist as members of one of four populations which we term R2, R3, R6 and R9, the R indicating the right family and the number indicating the equivalent stirring speed (to the closest 1000 rev./min) used for the coarse adjustment of molecular length (DNA concentration = 50 μg/ml.). Hence the R2 population was purified directly from right halves, while the R3, R6 and R9 populations were purified after the right halves had been further fragmented at 3000, 6000 and 9000 rev./min (Table 2).

The fragments in each of these populations were further subdivided by zone sedimentation in sucrose gradients with results which are shown in Figure 6. The fractions collected after each sedimentation were assayed for the activity of the appropriate gene combinations given in Table 2. The intercept of the abscissa with that portion of an activity curve exhibiting increasing activity with increasing radial

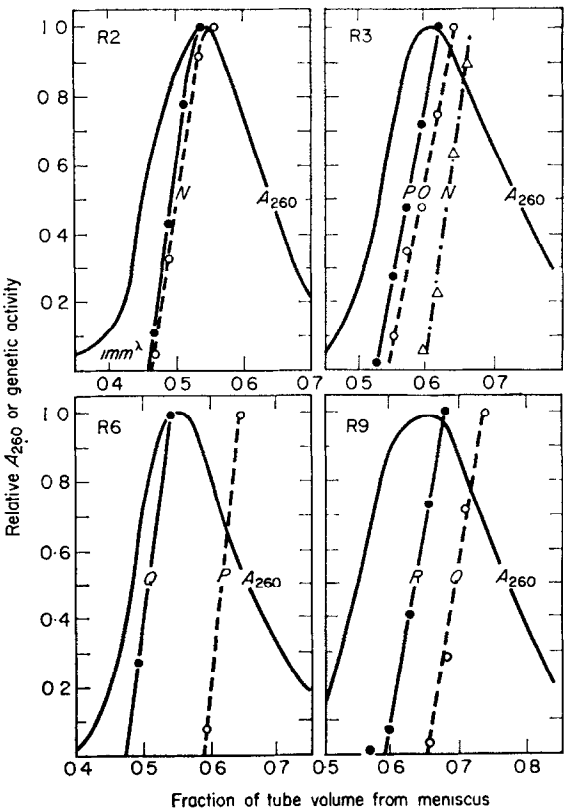

FIG. 6. Fine adjustment of molecular length by zone sedimentation.

The R2, R3, R6 and R9 populations (100 μg of DNA in 0·5 ml. of 0·001 M-EDTA, 0·01 M-Tris·HCl, pH 7·1) were layered on to 26 ml. of a 5 to 20% sucrose gradient in 0·317 M-CsCl, 0·001 M-EDTA, 0·01 M-Tris·HCl (pH 7·1), and centrifuged in a SW25.1 rotor at 25,000 rev./min and at 4 to 5°C for 10·2, 13·6, 14·9 and 19·2 hr, respectively. Fractions of 0·5 ml. were collected by upward displacement to minimize contamination of small with larger fragments, and assayed for gene content as indicated in Table 1. The results are given as relative plaque-forming units/ml. and only that portion of the curve exhibiting increasing activity with increasing radial distance is depicted, to simplify the figures. The $A_{260\,nm}$ traces (——) were obtained as in Fig. 2.

Sedimentation coefficients were determined as described in Experimental Procedure. The values of $S^0_{20,w}$ assigned to DNA at 0·5 on the abscissa of *R2*, *R3*, *R6* and *R9* are 23·2, 17·3, 15·5 and 11·0 s, respectively.

distance (the only portion shown in Fig. 6) indicates the point of division where all fractions to the right include fragments exhibiting activity for the gene in question, while fractions to the left do not. These curves serve as markers which allow one to correlate the different distributions and to estimate the resolution of the fractionation.

(b) *Molecular lengths of the fragments*

One can also correlate the distributions shown in Figure 6 by comparing their molecular lengths. We have done this by determining the $S^0_{20,w}$ of the DNA in one fraction (usually that containing the peak), and then calculating the $S^0_{20,w}$ for DNA in the other fractions from the distances sedimented relative to that for the DNA of known $S^0_{20,w}$ (see Experimental Procedure, section (b)). The molecular lengths of the

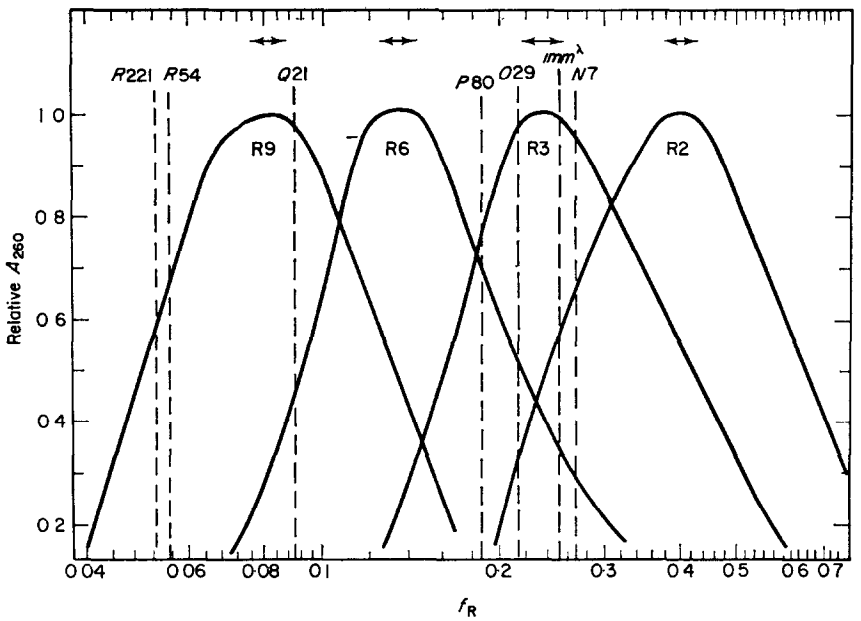

FIG. 7. The molecular length distributions for the fragments in the R2, R3, R6 and R9 groups. See the text for an explanation of f_R and the gene positions.

DNA were calculated from these values of $S^0_{20,w}$ according to equation (1). These lengths represent the distance from the right-hand end of λ DNA to the broken end of the fragment, and are expressed as the fraction of the length of whole λ DNA measured from the right-hand end (f_R). When applied to each of the curves in Figure 6, this procedure yields the results shown in Figure 7.

The molecular lengths were plotted on a logarithmic scale so that the 0·5 ml. fractions of each gradient would occupy approximately the same space (indicated by the double-ended arrow above each peak) on the graph. This plot emphasizes that while each fraction exhibits about the same percentage variation in molecular length, the absolute range per fraction increases proportionately with the length. The overlap between the four gradients is sufficient to ensure representation of all sequences in the λ DNA molecule located between $f_R = 0{\cdot}04$ and 0·65. Smaller fragments have been made by stirring at higher speed, but we have not investigated their properties.

(c) *Gene position*

Gene positions were determined by a second zone sedimentation of the DNA in those fractions of Figure 6 which first exhibit activity for the gene in question. The results are presented in Figure 8.

We wish to determine from these data the molecular length of the shortest fragment containing a given gene, this length representing the distance from the right end of λ DNA to the gene. The length of the DNA at the peak of the activity curve for the gene in question is larger than the desired minimal length. This is so because the first fractionation (Fig. 6) is imperfect, as is obvious from the displacements observed in Figure 8 between activity curves in the same gradient, or between the curve for a given activity and the corresponding $A_{260\,nm}$ trace.

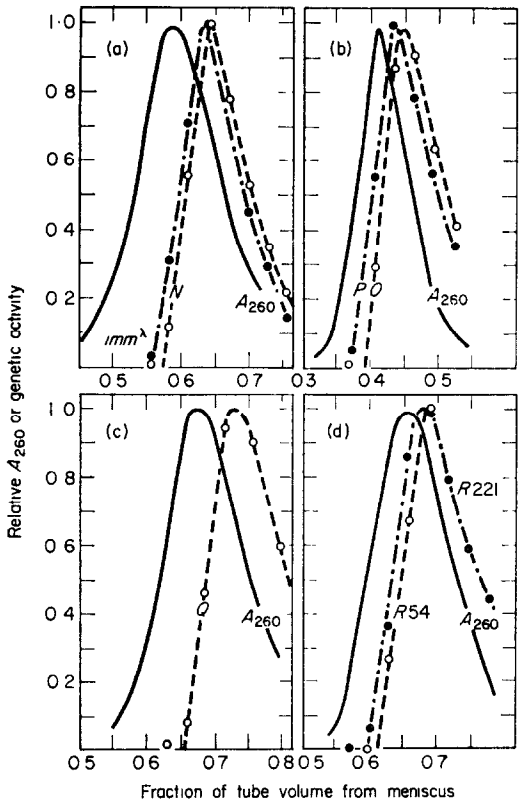

FIG. 8. Determination of gene positions by further fine adjustment of molecular lengths.

Four fractions obtained from the first zone sedimentation (Fig. 6) were each dialyzed (0·001 M-EDTA, 0·01 M-Tris·HCl, pH 7·1), concentrated by rotary evaporation, and 3 μg of DNA in 0·1 ml. then layered on to 4·6 ml. of the sucrose gradient defined in Fig. 6. The fractions used, the times of sedimentation in the SW39 rotor at 39,000 rev./min and 4 to 5°C, and the $S^0_{20,w}$ value for the DNA in the peak (determined by band sedimentation) are:

(a) fraction from R3 located at 0·595; 4·1 hr; 20·8 s;

(b) first fraction showing both *O* and *P* activities in R3-type zone sedimentation (not shown in Fig. 6, but comparable to fraction at 0·545 in R3); 3·6 hr; 19·6 s;

(c) fraction from R9 located at 0·655; 7·6 hr; 14·4 s;

(d) fraction from R9 located at 0·566; 7·6 hr; 12·6 s.

The gene activities are represented on the ordinate as in Fig. 6, *N*, *imm*$^{\lambda}$, *O*, *P* and *Q* being assayed as indicated there. The assay designated by *R*54 is the standard assay for *R* in which the helper phage was $\lambda imm^{434}R54{,}60$ (see Table 1). In the *R*221 assay, the helper phage was $\lambda cII2002$-*R*221 (Thomas *et al.*, 1967).

By contrast, linear extrapolation of the ascending side of an activity curve backward to the abscissa indicates a molecular length smaller than the desired minimal length; the zone sedimentation of a homogenous population of DNA yields a distribution in which such an extrapolate and the peak occupy appreciably different positions. The molecular lengths established by the extrapolated and peak positions of the genetic activity curves in Figure 8 therefore give a range of values which includes the desired minimal length.

A better determination of the minimal length can be made by defining the position of the peak of a homogeneous DNA population the trailing edge of which extrapolates to the same position on the abscissa as the above extrapolate for the curve of genetic

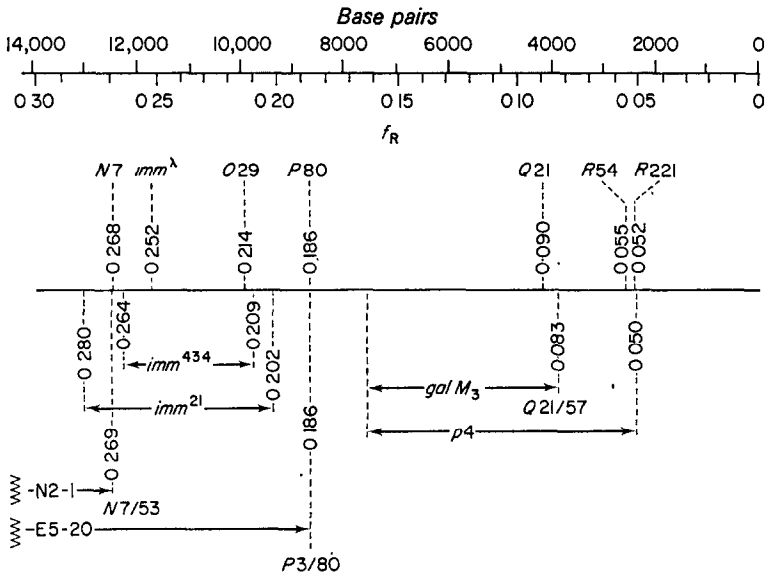

FIG. 9. Comparison of fragment and electron microscopic mapping.

The positions of the amber mutations and the left boundary of *imm*$^\lambda$ determined by fragment mapping are given above the lower horizontal line; the boundaries of deleted segments in λ variants determined by electron microscopic mapping appear below this line. The designation of the deleted segments (i.e. the symbol associated with each horizontal double-ended arrow) and the boundary positions are taken from the review by Davidson & Szybalski (1971). The symbol *N*7/53 at the right boundary of the *N*2-1 deletion indicates that *N*7$^+$ cannot be rescued from such phage, but that *N*53$^+$ can; *P*3/80 and *Q*21/57 should be interpreted in the same way. The scale of base pairs derives from the f_R scale and the 46,500 base pairs in whole λ DNA (Davidson & Szybalski, 1971).

activity. In five different experiments, zone sedimentation of whole λ DNA at low concentrations (0·1 to 1·0 μg/ml. in the initial zone) yielded a symmetrical zone in which the radial distance between the peak and the extrapolate of its trailing edge was 2·2 ± 0·3 times the width of the initial sample layered on the gradient. As almost all of this spreading is due to manipulations occurring before and after centrifugation, differences of zone width resulting from differences in time and rate of diffusion for the examples given in Figure 8 are small enough to be ignored. We, therefore, determine the position of the peak for molecules having the desired minimal length by adding to the extrapolated position for the activity curves, 2·2 times the width of the initial layer; e.g. this meant adding 0·048 to the value of the extrapolate for *Q* in Figure 8(c) (0·655) to obtain a value of 0·703. The molecular length of the DNA at this position was then calculated as described in Experimental Procedure. The resulting values are given in Figure 9. These values are very close (± 4%) to the midpoint of the range indicated in the previous paragraph.

4. Discussion

(a) *Accuracy and nature of the genetic mapping*

How accurate are the values in Figure 9? The only comparable physical mapping of genetic loci is the electron micrographic mapping of large chromosomal alterations. Such alterations of the λ genome have been isolated in sufficient numbers so that loci very close to the point mutations represented in Figure 9 have been mapped. The data for the comparisons given in the following paragraphs were taken from the summary

of electron micrographic mapping prepared by Davidson & Szybalski (1971), and are shown in Figure 9.

Gene *N*. A locus in *N* between mutations *N*7 and *N*53 has been mapped at $f_R = 0{\cdot}269$. This is in excellent agreement with our value of 0·268 for the *N*7 locus. The range of error that we expect is $\pm$ 6% of the determined value of f_R†, and therefore varies from $\pm$ 0·016 for *N* to $\pm$ 0·003 for *R*.

imm$^{\lambda}$. The locus termed *imm*$^{\lambda}$ on our map should be very close to the left boundary of the λ DNA deleted in λ *imm*^{434} (the segment designated *imm*^{434} in Fig. 9). This conclusion derives from our assay of *imm*$^{\lambda}$ which yields phage with the immunity of λ by recombination between a fragment and the DNA of the λ *imm*^{434} helper phage. We suppose that for the smallest fragments with *imm*$^{\lambda}$ activity such recombination occurs at the λ sequences located just to the left of the *imm*^{434} left boundary. Even if it were possible for a fragment-end created by breakage to the right of this boundary to recombine with λ *imm*^{434}, the fragment must contribute the operator–promoter sequence ($o_L p_L$) controlling leftward transcription in λ, and this lies just to the right of the *imm*^{434} left boundary (Blattner, Boettiger & Dahlberg, 1971). The value, $f_R = 0{\cdot}264$, given for this boundary by Davidson & Szybalski (1971) results from the work of Westmoreland, Szybalski & Ris (1969); Simon, Davis & Davidson (1971) place it at $f_R = 0{\cdot}260$. Our value of 0·252 for *imm*$^{\lambda}$ is therefore in good agreement with the above expectation.

Gene *O*. This gene has not been mapped by electron microscopy but should lie to the left of *P* and to the right of the right boundary of *imm*^{21} which has been mapped at $f_R = 0{\cdot}202$ (value given by Davidson & Szybalski, 1971, from work of Westmoreland *et al.*, 1969) and 0·205 (Simon *et al.*, 1971). Our value of 0·214 for *O*29 is to the wrong side of these map positions but is within our experimental error of either. The map positions for six identical chromosomal alterations reported by the two groups active in electron microscopic mapping (see Davidson & Szybalski, 1971) indicates differences of *f* in the range 0·001 to 0·010 ($\sigma = 0{\cdot}0023$), which may also account for some of the above discrepancy.

Genes *P* and *Q*. Loci in *P* (between mutations *P*3 and *P*80) and in *Q* (between *Q*21 and *Q*57) have been mapped at $f_R = 0{\cdot}186$ and 0·083, respectively, in agreement with our values of 0·186 for *P*80 and 0·090 for *Q*21. The difference in the *Q* values can be attributed to the unknown distance between the *Q* 21 and *Q*57 mutations (e.g. a Δf_R of 0·01 is sufficient to code for 155 amino acids).

Gene *R*. This gene has not been mapped by electron microscopy but at least part of it is thought to lie within the *p*4 segment (Fig. 9) deleted in $\lambda p4$, since *R*5$^+$ cannot be rescued from this phage (I. Herskowitz, cited by Fiandt, Hradecna, Lozeron & Szybalski, 1971). The position of the right boundary of *p*4 at $f_R = 0{\cdot}050$ is therefore consistent with our localization of *R*54 and *R*221 at 0·055 and 0·052, respectively. The order of these two loci on our physical map corresponds to their order on the genetic linkage map (Naha, 1966; Thomas *et al.*, 1967; J. Champoux, personal communication), the mutations mentioned in this article exhibiting the sequence —*R*54—(*R*5, *R*60)

† This range of error is a function of the following characteristics: the accuracy of the sedimentation coefficient and the molecular length calculated from it (Experimental Procedure, section (b)(vi) and (vii)); the size and position of the fractions in the sucrose gradient; the accuracy of the genetic activities and hence of the extrapolate to zero activity; and the correction of the extrapolated value explained in Results, section (c). Under our conditions, the composite of these effects leads to an estimated range of error of $\pm$6%. The range of observed values for three measurements of the *R*54 site was $\pm$5% of the mean f_R value.

—*R*221—cohesive site, with at least four other *R* mutations having been mapped to the left of *R*54. The difference between the positions of *R*54 and *R*221 ($\Delta f_R = 0{\cdot}003$) is also consistent with the small size of the *R* gene which is known to contain 480 base pairs (Black & Hogness, 1969), corresponding to $\Delta f_R = 0{\cdot}0103$.

Implicit in our determination of f_R for a given marker is the assumption that there is no significant variation in the efficiency of the genetic assay (i.e. plaque-forming units per fragment) as the fragment length increases beyond the f_R value for the marker. The validity of this assumption is indicated by the observation that the efficiency of assay for the *R*54 marker located at $f_R = 0{\cdot}055$ increases only slightly (approx. 1% per $\Delta f_R = 0{\cdot}01$) as the fragment length increases from $f_R = 0{\cdot}13$ to 0·40. If this rate does not increase as the fragment length more closely approaches the f_R value for the marker, then the change in efficiency calculated for the lengths included in the extrapolations shown in Figure 8 is insignificant. The generally excellent agreement between our results and the electron micrographic map provides a further indication that variation in efficiency with fragment length is not a significant factor.

The agreement between the two physical maps also provides substantiation of equation (1). Indeed the data in Figure 9, when added to that presented in Figure 3, provide the most substantial set of data relating $S^0_{20,w}$ to molecular weight (M) for duplex DNA in the range $M = 0{\cdot}3$ to 31×10^6 daltons, and indicate the validity of the equation, $S^0_{20,w} = KM^{0{\cdot}350}$, used to generate equation (1)†.

It should be noted that genetic loci can be mapped by the general method given here without removing the internal fragments before zone sedimentation. This is because the internal fragments are inactive in the helper phage assay (see legend, Fig. 4), a cohesive site being a necessary condition for such activity (Kaiser & Inman, 1965). This more rapid genetic mapping procedure was used previously to yield a preliminary map giving the approximate positions of *N*, *O*, *P* and *Q* (Hogness, Doerfler, Egan & Black, 1966); these agree well with the present more accurate and extensive results obtained with fragments which can also be used for chemical mapping *because* the internal fragments have been removed.

(b) *Characteristics pertaining to chemical mapping*

(i) *Single-strand breaks*

The fragments should be essentially free of single-strand breaks to maximize their use in the mapping of strand-specific characteristics such as the poly(rG) binding sites analyzed in the following paper (Champoux & Hogness, 1972). Less than one strand in five of whole duplex λ DNA contains a break (see Experimental Methods), and this frequency should decrease with decreasing fragment size unless additional single-strand breaks are introduced during formation and isolation. This does not appear to be the case. We have examined the sedimentation distribution of the strands from isolated fragments (mean $f_R = 0{\cdot}138$) by band sedimentation in 0·1 N-

† If T7 DNA is accepted as the best primary standard (Freifelder, 1970) and K calculated from its molecular weight ($25{\cdot}2 \times 10^6$ daltons) and $S^0_{20,w}$ (32·0 S), one obtains a value of 0·0822, quite consistent with the value of 0·0823 computed from the data for λ DNA ($M = 30{\cdot}8 \times 10^6$, Davidson & Szybalski (1971); $S^0_{20,w} = 34{\cdot}4$ S, Freifelder (1970) and our results), and with that obtained from the composite of the data in Figs 3 and 9. This value is to be compared with 0·0833 found by Leighton & Rubinstein (1969) and 0·080 by Burgi & Hershey (1963), both groups using 0·35 for the exponent of M, and including DNA's of higher molecular weight than considered here. Studier's (1965) equation, $S^0_{20,w} = 0{\cdot}0882\ M^{0{\cdot}346}$, is in good agreement with our equation for molecular weights in the range of T7 and λ DNA, but is less favorable at the lower molecular weights given in Fig. 3.

NaOH, 0·9 M-NaCl without observing any excess of slowly sedimenting DNA over that observed during sedimentation of the corresponding duplex population; and the $S^0_{20,w}$ for the peak of the strand distribution is within experimental error of that predicted from the $S^0_{20,w}$ for the peak of the duplexes (Studier, 1965).

(ii) *Length distribution of isolated fragment populations*

The degree of overlap in the length distributions of adjacent fractions from the sucrose gradients (Figs 6 and 7) determines the level of resolution available at that stage of purification. As a measure of this overlap, we have used the percentage of fragments in a given fraction which has lengths equal to or longer than the mean length of the DNA in the adjacent fraction further down the tube. Estimating this percentage from the distribution observed when the DNA in a given fraction is resedimented (e.g. as in Fig. 8†), we obtain values of $25 \pm 5\%$ for adjacent fractions the mean f_R values of which differ by 12% (Fig. 7). The significance of such an overlap depends upon the chemical characteristic in question and should be considered separately for each case (e.g. see Champoux & Hogness, 1972). We mention it here to point out a limitation of the method which can be modified only by additional zone sedimentation (as was done for the analysis of genetic loci (Fig. 8)), or by applying fractionation procedures of greater resolving power than zone sedimentation.

(iii) *Fragments from the left family*

The fragments of the left family can be similarly isolated; indeed the basic components (unlabeled left halves and bromouracil-labeled right halves) for such isolation automatically become available in preparing the corresponding components for isolation of members of the right family. At present, only those fragments in the left family with lengths comparable to the fragments obtained from the *R*2 subset have been isolated. These have been used in combination with the right fragments defined in Figures 6 and 7 to determine the topography of the λ genome with respect to base composition and to the position and orientation of the specific sequences generating the poly(rG) binding sites (Champoux & Hogness, 1972).

We thank Mrs Janet Bodes Neal and Mr David Loskotoff for their invaluable technical assistance, and Dr Mark Pearson for his helpful suggestions and for the development of the microcell used in the Gilford spectrophotometer. This research was supported by grants from the National Institutes of Health and the National Science Foundation. One of us (J. B. E.) thanks the Jane Coffin Childs Foundation for Medical Research for their fellowship support and personal interest.

† Two methods were used. In one, the shape of the distribution of the resedimented DNA (e.g. Fig. 8(c)) was approximated by the sum of a set of model distributions (usually 7), each having the characteristics of the distribution observed for homogeneous DNA (see Results, section (c)), and equally spaced along the gradient with the peak of the central model distribution located at the peak position of the actual distribution. The frequencies of the model distributions were varied to obtain the best fit to the actual distribution, and after converting these mass frequencies to number frequencies, the desired percentage was obtained from the sum of those model frequencies representing DNA with f_R value equal to or larger than the mean f_R value of the adjacent fraction. The results obtained by this method are in good agreement with those obtained when the DNA in a given fraction from Fig. 6 was subject to boundary sedimentation in the analytical ultracentrifuge and the distribution of sedimentation coefficients (and therefore of f_R) determined by analysis of the boundary (Schumaker & Schachman, 1957).

REFERENCES

Appleyard, R. (1954). *Genetics*, **39**, 440.

Baldwin, R. L. (1971). In *Procedures in Nucleic Acid Research*, ed. by G. L. Cantoni & D. R. Davies, vol. 2, p. 355. New York and London: Harper & Row.

Baldwin, R. L., Barrand, P., Fritsch, A., Goldthwait, D. A. & Jacob, F. (1966). *J. Mol. Biol.* **17**, 343.

Black, L. W. & Hogness, D. S. (1969). *J. Biol. Chem.* **244**, 1966.

Blattner, F. R., Boettiger, J. K. & Dahlberg, J. E. (1971). *Fed. Proc.* **30**, 1315.

Bruner, R. & Vinograd, J. (1965). *Biochim. biophys. Acta*, **108**, 18.

Burgi, E. & Hershey, A. D. (1963). *Biophys. J.* **3**, 309.

Campbell, A. (1971). In *The Bacteriophage Lambda*, ed. by A. D. Hershey, p. 13. Cold Spring Harbor, New York: Cold Spring Harbor Laboratories.

Campbell, A. (1961). *Virology*, **14**, 22.

Casjens, S., Hohn, T. & Kaiser, A. D. (1970). *Virology*, **42**, 496.

Champoux, J. & Hogness, D. S. (1972). *J. Mol. Biol.* **71**, 383.

Crothers, D. M. & Zimm, B. H. (1965). *J. Mol. Biol.* **12**, 525.

Davidson, N. & Szybalski, W. (1971). In *The Bacteriophage Lambda*, ed. by A. D. Hershey, p. 45. Cold Spring Harbor, New York: Cold Spring Harbor Laboratories.

Doerfler, W. & Hogness, D. S. (1968). *J. Mol. Biol.* **33**, 365.

Eigner, J. & Doty, P. (1965). *J. Mol. Biol.* **12**, 549.

Fiandt, M., Hradecna, Z., Lozeron, H. A. & Szybalski, W. (1971). In *The Bacteriophage Lambda*, ed. by A. D. Hershey, p. 329. Cold Spring Harbor, New York: Cold Spring Harbor Laboratories.

Freifelder, D. (1970). *J. Mol. Biol.* **54**, 567.

Hearst, J. E. (1962). *J. Mol. Biol.* **4**, 415.

Hershey, A. D., Burgi, E. & Ingraham, L. (1963). *Proc. Nat. Acad. Sci., Wash.* **49**, 748.

Hogness, D. S. (1966). *J. Gen. Physiol.* **49**, 29.

Hogness, D. S., Doerfler, W., Egan, J. B. & Black, L. W. (1966). *Cold Spr. Harb. Symp. Quant. Biol.* **31**, 129.

Hogness, D. S. & Simmons, J. R. (1964). *J. Mol. Biol.* **9**, 411.

International Critical Tables (*1926 to 1933*). Ed. by E. W. Washburn. New York: McGraw-Hill Book Co., Inc.

Kaiser, A. D. & Hogness, D. S. (1960). *J. Mol. Biol.* **2**, 392.

Kaiser, A. D. & Inman, R. B. (1965). *J. Mol. Biol.* **13**, 78.

Kaiser, A. D. & Jacob, F. (1957). *Virology*, **4**, 509.

Leighton, S. B. & Rubinstein, I. (1969). *J. Mol. Biol.* **46**, 313.

Lyons, P. A. & Riley, J. F. (1954). *J. Amer. Chem. Soc.* **76**, 5216.

Martin, R. G. & Ames, B. N. (1961). *J. Biol. Chem.* **236**, 1372.

Naha, P. M. (1966). *Virology*, **29**, 676.

Nandi, U. S., Wang, J. C. & Davidson, N. (1965). *Biochemistry*, **4**, 1687.

Schumaker, V. N. & Schachman, H. K. (1957). *Biochim. biophys. Acta*, **23**, 628.

Simon, M. N., Davis, R. W. & Davidson, N. (1971). In *The Bacteriophage Lambda*, ed. by A. D. Hershey, p. 313. Cold Spring Harbor, New York: Cold Spring Harbor Laboratories.

Studier, F. W. (1965). *J. Mol. Biol.* **11**, 373.

Sussman, R. & Jacob, F. (1962). *C. R. Acad. Sci., Paris*, **254**, 1517.

Thomas, R., Leurs, C., Dambly, C., Parmentier, D., Lambert, L., Bracher, P., Lefebvre, N., Mousset, S., Porcheret, J., Szpirer, J. & Wauters, D. (1967). *Mutation Res.* **4**, 735.

Vinograd, J., Bruner, R., Kent, R. & Weigle, J. (1963). *Proc. Nat. Acad. Sci., Wash.* **49**, 902.

Wang, J. C., Nandi, U. S., Hogness, D. S. & Davidson, N. (1965). *Biochemistry*, **4**, 1697.

Westmoreland, B. C., Szybalski, W. & Ris, H. (1969). *Science*, **163**, 1343.

Wu, R. & Taylor, E. (1971). *J. Mol. Biol.* **57**, 491.

Yanofsky, C. & Ito, J. (1966). *J. Mol. Biol.* **21**, 313.